Physics of the Earth and Planetary Interiors 180 (2010) 209–214

Contents lists available at ScienceDirect

Physics of the Earth and Planetary Interiors

journal homepage: www.elsevier.com/locate/pepi

Effect of site degeneracies on the spin crossovers in (Mg, Fe)SiO_3 perovskite

Koichiro Umemoto[a,c,*], Han Hsu[b,c], Renata M. Wentzcovitch[b,c]

[a] Department of Geology and Geophysics, University of Minnesota, Minneapolis, MN 55455, USA
[b] Department of Chemical Engineering Materials Science, University of Minnesota, Minneapolis, MN 55455, USA
[c] Minnesota Supercomputing Institute, University of Minnesota, Minneapolis, MN 55455, USA

ARTICLE INFO

Article history:
Received 29 April 2009
Received in revised form 17 October 2009
Accepted 29 October 2009

Guest Editors
Kei Hirose
Thorne Lay
David Yuen

Editor
G. Helffrich

Keywords:
Spin crossover
Ferrous iron
Perovskite
Lower mantle
First principles

ABSTRACT

We investigate by first principles several aspects of the spin crossover of ferrous iron (Fe^{2+}) between the high-spin (HS), intermediate-spin (IS), and low-spin (LS) states in $MgSiO_3$ perovskite under pressure. First, we investigate the effect of site degeneracy intrinsic to LS and IS states of iron. We show that the entropy owing to this effect (site entropy) significantly increases the fraction of LS irons and reduces the crossover onset pressure, especially at high temperatures. Even including the effect of site entropy, the fraction of IS irons in the lower mantle or in the laboratory is predicted to be negligible. We also show that the effect of the crossover on equation-of-state parameters is probably undetectable at any temperature. Although we address only ferrous iron in only one atomic configuration and results are specific to this situation, our results suggest that the effect of the crossover on the bulk modulus derived from direct sound speed measurements could perhaps be more noticeable below room temperature. However, at mantle conditions the bulk sound speed should hardly be affected by the crossover.

1. Introduction

Iron-bearing magnesium silicate perovskite, (Mg, Fe)SiO_3, is believed to be the major mineral of Earth's lower mantle. The presence of iron in perovskite is known to affect several lower mantle properties: elastic and seismic properties (Kiefer et al., 2002; Li et al., 2005; Tsuchiya and Tsuchiya, 2006; Stackhouse et al., 2007), the post-perovskite transition pressure (Caracas and Cohen, 2005; Mao et al., 2005; Ono and Oganov, 2005; Stackhouse et al., 2006; Tateno et al., 2007) and electrical and thermal conductivities (Burns, 1993; Katsura et al., 1998; Xu et al., 1998; Badro et al., 2004), to mention a few. Therefore the spin states of ferrous (Fe^{2+}) and ferric (Fe^{3+}) irons have been intensively studied experimentally and theoretically. However, there are some discrepancies between these studies.

Experimentally, Badro et al. (2004) reported two distinct spin transitions: the first from the high-spin (HS) state to a mixed-spin (MS) state at ~70 GPa and a subsequent one to the low-spin (LS) state at ~120 GPa. Li et al. (2004) reported a gradual spin transition through the intermediate-spin (IS) state which was not completed up to 100 GPa. A gradual spin transition was also reported by Jackson et al. (2005), suggesting that ferric iron was responsible for the transition which ended around 70 GPa. Lin et al. (2008) and McCammon et al. (2008) reported that ferrous iron should exist predominantly in the IS state at lower mantle condition. Several theoretical calculations showed that ferric iron undergoes a spin transition at lower mantle pressures, while the transition pressure for ferrous iron was calculated to be outside lower mantle's pressure range (Cohen et al., 1997; Li et al., 2005; Hofmeister, 2006; Zhang and Oganov, 2006; Stackhouse et al., 2007; Bengtson et al., 2008). Recently we showed that the spin transition pressure of ferrous iron depends strongly on magnesium-iron ordering, resulting in a variety of spin crossover pressures (Umemoto et al., 2008). For the lowest-energy configuration, the iron-(1 1 0) configuration, the crossover pressure was found to be in the pressure range of the lower mantle. We also showed that a displacement of iron from the preferred magnesium site, leading to a change in the iron coordination number, is vital for the occurrence of the spin crossover (Fig. 1(a)). Because of the mirror plane on which magnesium and HS irons exist, upward and downward displacements of LS and IS irons in Fig. 1(a) are symmetrically identical. These two equivalent displacements give an additional contribution to the entropy

* Corresponding author at: Department of Geology and Geophysics, University of Minnesota, Minneapolis, MN 55455, USA. Tel.: +1 612 625 8597; fax: +1 612 626 7246.
E-mail addresses: umemoto@cems.umn.edu (K. Umemoto), hsuhan@cems.umn.edu (H. Hsu), wentzcov@cems.umn.edu (R.M. Wentzcovitch).

0031-9201/$ – see front matter © 2009 Elsevier B.V. All rights reserved.
doi:10.1016/j.pepi.2009.10.014

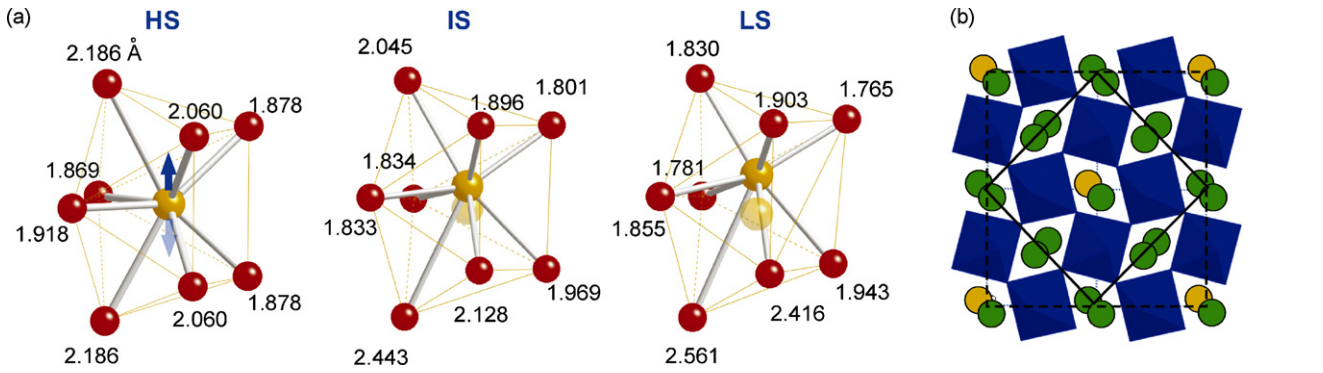

Fig. 1. (a) Local atomic structure around HS, IS, LS irons at 120 GPa optimized for $Mg_{0.875}Fe_{0.125}SiO_3$. Numbers denote Fe-O bond lengths in Å. Pale spheres represent symmetrically equivalent irons for IS and LS states. (b) Atomic structure used in the present calculation. Green and ocherous spheres denote magnesiums and irons, respectively. The solid box represents the supercell with 40 atoms. The dashed box denotes the supercell with 80 atoms used for a test for validity of an assumption of the ideal solid solution (see text).

intrinsic to LS and IS states. We refer to this contribution as *site entropy* hereafter. This additional entropy contribution is expected to further stabilize the LS and IS states at high temperatures. Here we investigate the effect of site degeneracy on the entropy and on the spin crossover in $Mg_{0.875}Fe_{0.125}SiO_3$. This iron concentration is close to that expected in the lower mantle.

2. Theoretical approach and computational method

The atomic structure of $Mg_{0.875}Fe_{0.125}SiO_3$ used in the present calculations is shown in Fig. 1(b). The 40-atom supercell contains one iron. Our thermodynamic treatment of the MS state assumes an ideal solid solution of pure HS, IS, and LS states, which is realistic for this atomic configuration. The fraction of each spin state is then calculated by either of the following approaches: (1) from a thermodynamic treatment considering explicitly all contributions to the Gibbs free energy or (2) directly from the partition function. The second approach is more convenient when the electronic/magnetic entropy is more complicated, for instance, when the inclusion of highly excited electronic state or spin-orbit effects are essential, or the solid solution is not ideal. These two approaches are equivalent. Here we disregard vibrational effects which were considered in previous studies of ferropericlase (Wu et al., 2009; Wentzcovitch et al., 2009). They are essential for predicting free energies, thermodynamics properties, and should superpose to the effects calculated here. Our goal here is to investigate the magnitude of a particular phenomenon that should not be strongly affected by (quasi)harmonic vibrations. However, anharmonic fluctuations in the iron position could have an unpredictable effect.

2.1. Computational details

Calculations were performed using the local-density approximation (LDA) (Perdew and Zunder, 1981). The pseudopotentials for Fe, Si, and O were generated by Vanderbilt's method (Vanderbilt, 1990). The valence electronic configurations used are $3s^2 3p^6 3d^{6.5} 4s^1 4p^0$, $3s^2 3p^1$, and $2s^2 2p^4$ for Fe, Si, and O. Core radii for all quantum numbers l are 1.8, 1.6, and 1.4 a.u. for Fe, Si and O. The pseudopotential for Mg was generated by von Barth-Car's method. Five configurations, $3s^2 3p^0$, $3s^1 3p^1$, $3s^1 3p^{0.5} 3d^{0.5}$, $3s^1 3p^{0.5}$, and $3s^1 3d^1$ with decreasing weights 1.5, 0.6, 0.3, 0.3, and 0.2, respectively, were used. Core radii for all quantum numbers l are 2.5 a.u.. The plane-wave cutoff energy is 40 Ry. The $2 \times 2 \times 4$ k-point mesh is used for the Brillouin zone sampling. We used variable-cell-shape molecular dynamics (Wentzcovitch, 1991; Wentzcovitch et al., 1993) for structural optimization under arbitrary pressures.

2.2. $n(P, T)$ from the free energy

Here we expand the approach developed by Tsuchiya et al. (2006) to calculate the fraction of LS iron in the MS state. We now include the IS state as well as the site entropy contribution to the free energy. The molar Gibbs free energy of the MS state, $G(n, P, T)$, is given by

$$G(n, P, T) = \sum_{\sigma=HS,IS,LS} n_\sigma(P, T) G_\sigma(P, T) + G^{mix}(P, T), \quad (1)$$

where n_σ and G_σ are the fraction and the Gibbs free energy of each spin state, respectively, and G^{mix} is the free energy of mixing of the ideal solid solution with three spin states. G^{mix} is

$$G^{mix} = k_B T X_{Fe} \sum_\sigma n_\sigma \log n_\sigma, \quad (2)$$

where X_{Fe} is the iron concentration. Disregarding vibrational effects, the molar Gibbs free energy of each component has three contributions:

$$G_\sigma = H_\sigma + G_\sigma^{mag} + G_\sigma^{site}. \quad (3)$$

The first term is the static enthalpy. The second term is the contribution from magnetic entropy. In the ideal solid solution formalism, the free energy of the HS or IS states does not depend on the spin coupling between irons. The magnetic entropy is then given simply by

$$G_\sigma^{mag} = -k_B T X_{Fe} \log(m_\sigma(2S_\sigma + 1)) \equiv -k_B T X_{Fe} \log M_\sigma, \quad (4)$$

where m_σ and S_σ are the orbital degeneracy and the spin quantum number for each spin state, respectively. The third term, G_σ^{site}, is the free energy contribution from site entropy:

$$G_\sigma^{site} = -k_B T X_{Fe} \log N_\sigma^{site}. \quad (5)$$

Here N_σ^{site} is the number of equivalent sites for each spin state, i.e., $N_{LS(IS)}^{site} = 2$ and $N_{HS}^{site} = 1$. Thus, for the HS state, $G_{HS}^{site} = 0$. The constraint on the fractions n_σ is

$$\sum_{\sigma=HS,IS,LS} n_\sigma = 1, \quad \text{or,} \quad n_{HS} = 1 - n_{IS} - n_{LS}. \quad (6)$$

In principle one should also include the vibrational free energy, but the focus here is to understand the effect of site degeneracy. The effect of vibrations will be the subject of future work. Therefore, n_{LS}

and n_{IS} are obtained by minimizing the free energy (in Eq. (1)) with respect to n_{LS} and n_{IS}. We then obtain:

$$n_{HS}(P,T) = \frac{M_{HS}}{M_{HS} + N_{LS}^{site} M_{LS} \exp(-(\Delta H_{LS})/(k_B T X_{Fe})) + N_{IS}^{site} M_{IS} \exp(-(\Delta H_{IS})/(k_B T X_{Fe}))}, \quad (7)$$

$$n_{LS(IS)}(P,T) = \frac{N_{LS(IS)}^{site} M_{LS(IS)}}{M_{HS}} \exp\left(-\frac{\Delta H_{LS(IS)}}{k_B T X_{Fe}}\right) n_{HS}, \quad (8)$$

where $\Delta H_{LS(IS)} \equiv H_{LS(IS)} - H_{HS}$.

2.3. $n(P,T)$ from the partition function

The partition function of this system is:

$$Z(V,T) = \sum_{\sigma=HS,IS,LS} w_\sigma \exp\left(-\frac{E_\sigma(V)}{k_B T}\right), \quad (9)$$

where $E_\sigma(V)$ is the total energy and $w_\sigma = M_\sigma N_\sigma^{site}$ is the degeneracy for each spin state. The fraction of each spin state is then readily obtained:

$$n_\sigma(V,T) = \frac{w_\sigma \exp(-(E_\sigma(V))/(k_B T))}{Z(V,T)}. \quad (10)$$

Change of variables then gives $n_\sigma(P,T)$.

3. Results and discussion

3.1. Stability of the IS state

We performed calculations in the HS, LS, and IS states. For the IS state, at first the total magnetic moment per unit cell was constrained to $2\mu_B$. But once the equilibrium position of iron was obtained, we allowed the magnetic moment to be relaxed and the IS state was found to remain in equilibrium. IS irons are displaced from the mirror plane, but their displacements are smaller than those of LS irons (Fig. 1). Fig. 2 shows the relative enthalpy of all spin states. The IS state has the highest enthalpy and is metastable in the entire pressure range of the mantle. This result is consistent with those of previous computational studies (Zhang and Oganov, 2006; Stackhouse et al., 2007; Bengtson et al., 2008). As shown later in Sec. 3.2 and 3.3, even including site and magnetic entropies, the fraction of the IS state remains negligible. The HS ↔ IS crossover at ~30 GPa was proposed to explain the increase to high value (> 3.5 mm/s) in the nuclear quadrupole splitting (QS) of ferrous iron observed in Mössbauer experiments (Lin et al., 2008; McCammon et al., 2008). This interpretation assumed that IS iron has a less symmetric electronic charge density than HS iron and produces larger electric field gradients at the nucleus. However, recent calculations (Bengtson et al., 2009; Hsu et al., 2009) indicated that IS ferrous iron has a small QS, i.e., < 1 mm/s. Hence, enthalpy and QS calculations do not support the proposed interpretation of Mössbauer data (Lin et al., 2008; McCammon et al., 2008). Although there are still several factors that need to be investigated and could affect these results and conclusions (vibrational entropy, anharmonicity, etc), so far computational studies unanimously suggest that the IS state is highly metastable and has small QS.

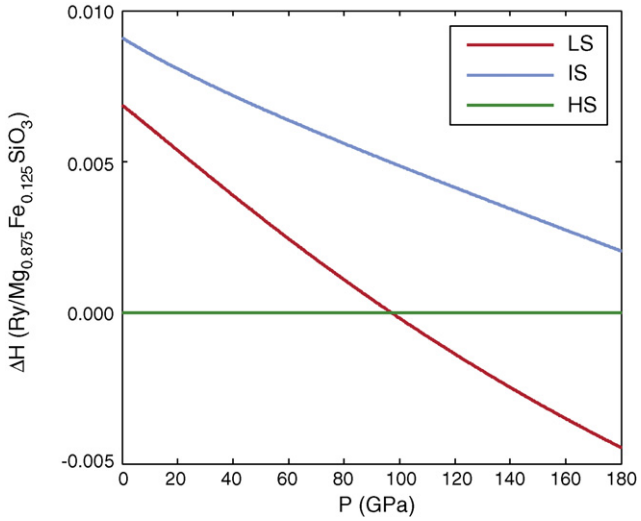

Fig. 2. Calculated enthalpies for LS and IS states with respect to the HS state.

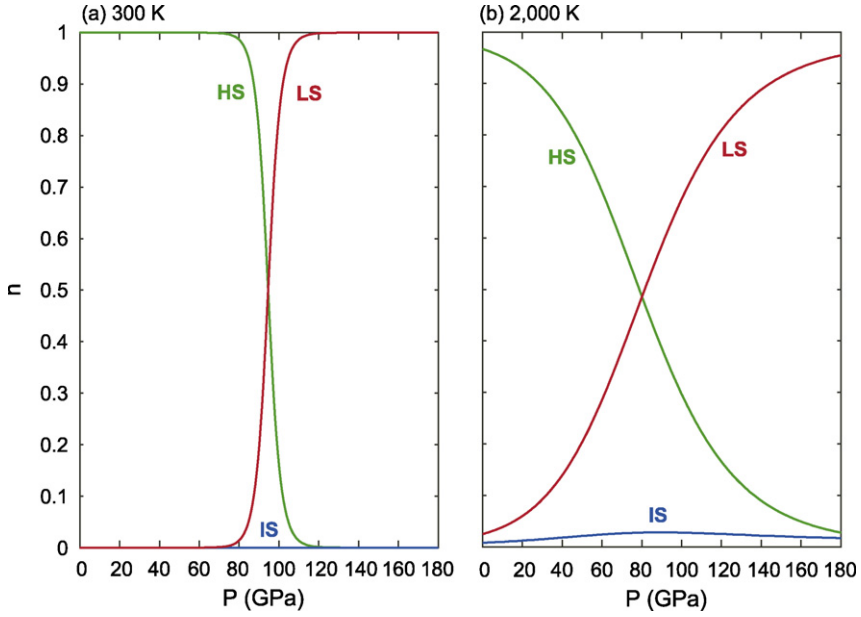

Fig. 3. Iron fractions in each spin state (n_{HS}, n_{IS}, and n_{LS}) at (a) 300 K and (b) 2000 K as result of site entropy only. Magnetic entropy was disregarded here.

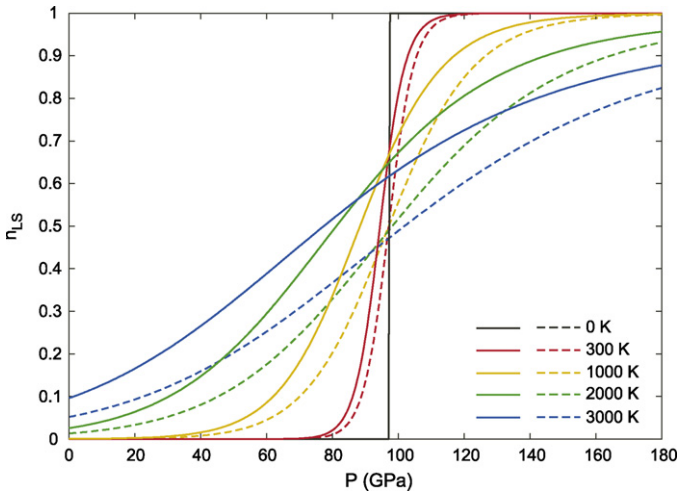

Fig. 4. LS iron fraction (n_{LS}) at several temperatures. Solid and dashed lines denote n_{LS} calculated with and without LS site entropy ($N_{LS}^{site} = 2$ and $N_{LS}^{site} = 1$), respectively. Magnetic entropy was disregarded here.

3.2. Effect of site entropy

In order to see the effect of site entropy clearly, we temporarily disregard the magnetic entropy term ($G_{\sigma}^{mag} = 0$ in Eq. (4)). Fig. 3 shows the fraction of each spin state at 300 and 2000 K. At 300 K n_{HS} and n_{LS} change very sharply, while at 2000 K they do so smoothly. Even with site entropy, n_{IS} is negligible at 300 K and still quite small at 2000 K, indicating that the IS state should scarcely occur in the lower mantle. Fig. 4 shows n_{LS} at several temperatures. Site entropy does not affect n_{LS} at 0 K, as expected. At finite temperatures it helps stabilize the LS state with respect to the HS state. Without site entropy, the HS ↔ LS crossover pressure (where $n_{LS} \simeq 0.5$) is 97 GPa at all temperatures (Fig. 4). The inclusion of site entropy changes this pressure to 95 GPa at 300 K, 88 GPa at 1000 K, 80 GPa at 2000 K, and 72 GPa at 3000 K. Therefore, at lower mantle temperatures, site entropy should decrease noticeably the onset of the spin crossover.

The effect of site entropy has been calculated in a 40-atom unit cell with a single iron ($Mg_{0.875}Fe_{0.125}SiO_3$), using an ideal solid solution model, i.e., disregarding the effects of correlation between iron displacements. For the particular atomic configuration considered here, indeed this effect is very small. This has been verified in a 80-atom supercell calculation (defined by the dashed line in Fig. 1 (b)). Two calculations with irons displaced in the same and in the opposite directions were performed in this cell. The enthalpy difference between these displacements leads to negligible difference in n_{LS} (less than 0.03). Hence, correlation between displacements of two LS irons is negligible and the ideal solid solution model is valid *for this particular iron configuration*. However, the ideal solid solution model is inappropriate for high iron concentrations and/or for other atomic configurations where irons are close to each other. In $FeSiO_3$ and in the iron-(1 1 0) configuration of (Mg, Fe)SiO_3 (Umemoto et al., 2008), displacements of LS irons are strongly correlated; all LS irons are displaced in the same direction. The enthalpy of configurations with irons displaced in opposite directions is considerably higher and these configurations are very unlikely. Those static calculations indicated that there is a tendency for iron clustering in (Mg, Fe)SiO_3 perovskite resulting in iron-rich and iron-poor regions (Umemoto et al., 2008). This clustering should reduce the number of structural degrees of freedom of LS iron by forcing them to displace in the same direction. Therefore the effect of site entropy is suppressed in iron-rich regions. In iron-poor regions, the static spin crossover pressure is higher than in iron-rich regions, but site entropy should decrease the crossover pressure and increase n_{LS} as shown in Fig. 4.

3.3. Effect of magnetic entropy

Now we include also magnetic entropy in the thermodynamic equilibrium calculation. It is known that in ferropericlase the magnetic entropy leads to a gradual spin crossover through a MS state at high temperatures (Sturhahn et al., 2005; Tsuchiya et al., 2006; Lin et al., 2007). We let $S_{HS} = 2$, $S_{IS} = 1$, and $S_{LS} = 0$ in Eq. (4). Since the electronic degeneracy of the d states is lifted in (Mg, Fe)SiO_3 (Umemoto et al., 2008), $m_{\sigma} = 1$ for the all spin states. In the IS state, the free energy has contributions from both magnetic and site entropies, but n_{IS} is still much smaller than n_{HS} and n_{LS}. Fig. 5(a) shows $n_{LS}(P, T)$ with magnetic and site entropies. Since $|M_{HS}| > |N_{LS}^{site}|$, the effect of magnetic entropy is stronger than that of site entropy. Nevertheless, we can still see a clear effect of site entropy by comparing n_{LS} calculated with and without the site entropy term in Fig. 5(a) and (b), respectively. Site entropy expands the stability field of the LS state, partially compensating the effect of magnetic entropy.

3.4. Effect of the spin crossover on volume and bulk modulus

The calculated compression curves of the HS, LS, and MS states are shown in Fig. 6. The corresponding equation-of-state parameters are given in Table 1. The compression curves are nearly parallel to the experimental data on samples with 15% iron concentration (Lundin et al., 2008) but volume is slightly underestimated

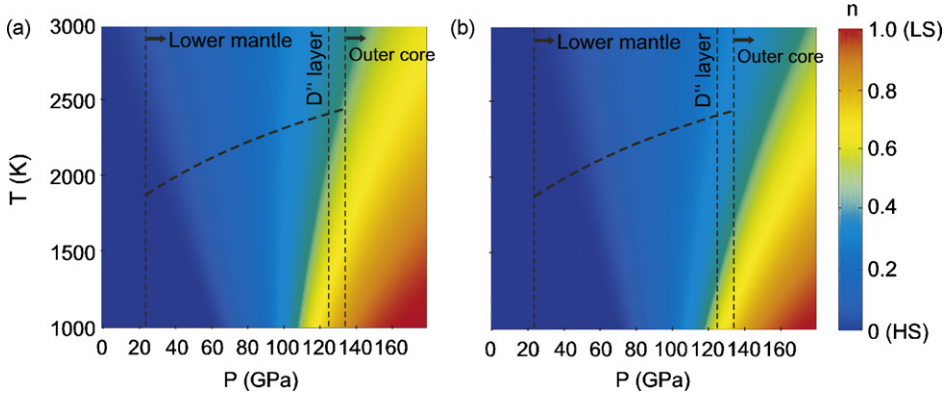

Fig. 5. LS iron fraction (n_{LS}) with magnetic entropy. In (a) the LS site entropy is included ($N_{LS}^{site} = 2$), while in (b) it is not included ($N_{LS}^{site} = 1$). Dashed lines denote a mantle geotherm derived by Brown and Shankland (1981).

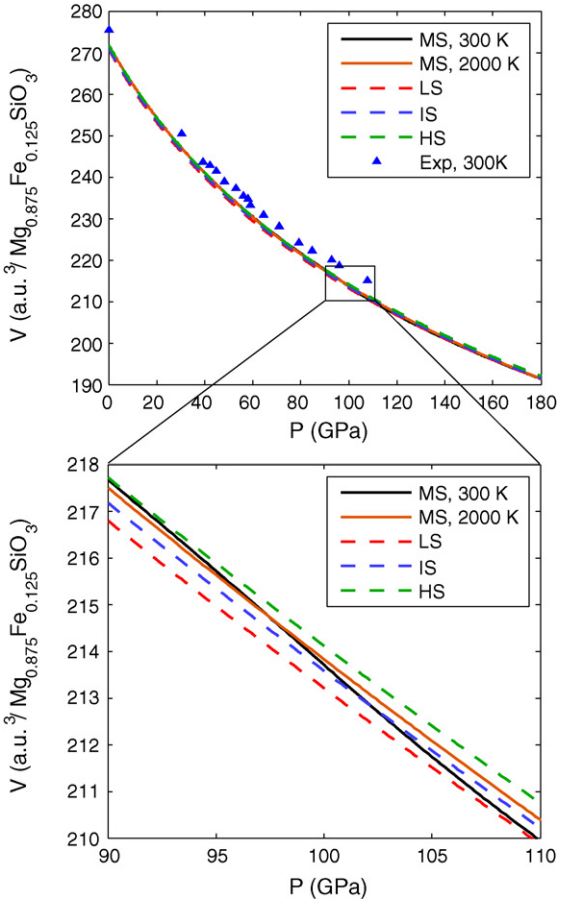

Fig. 6. Compression curves for the MS state at 300 and 2000 K and for HS, IS, and LS states. It should be noted that vibrational contribution to the free energy was not included here and volumes are underestimated. Experimental values for 15% iron concentration are taken from Lundin et al. (2008).

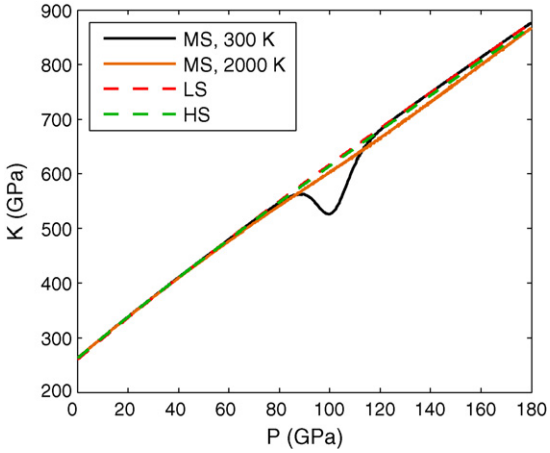

Fig. 7. Pressure dependence of the bulk modulus of the MS state at 300 and 2000 K and for the HS and LS states.

because vibrational effects have not been included. Volume of the MS state changes continuously between those of HS and LS states. At high temperatures relevant for the lower mantle the crossover is smooth and unnoticeable. Since the volume difference between the HS and LS states is quite small (~0.3%), the volume reduction during the spin crossover is difficult to be detected in view of experimental uncertainties (Lundin et al., 2008). This behavior is different from that of the spin crossover in ferropericlase (Lin et al., 2005; Tsuchiya et al., 2006; Fei et al., 2007; Wentzcovitch et al., 2009; Wu et al., 2009).

Finally, we investigate the effect of the spin crossover on the bulk modulus of *the particular atomic configuration we used*. In ferropericlase, direct sound velocity measurements and calculations showed an anomalous reduction of bulk modulus throughout the spin crossover (Crowhurst et al., 2008; Wentzcovitch et al., 2009; Wu et al., 2009). Fig. 7 shows the bulk modulus of the MS state at 300 K. At ~100 GPa its bulk modulus is reduced by ~16% with respect to those of the HS and LS states. However, at 2000 K, this effect is not very noticeable because of the broad crossover pressure range. Furthermore, (Mg, Fe)SiO_3 perovskite is expected to be a disordered solid solution, possibly with some iron clustering and with some ferric iron. The crossover pressure range in the real system is expected to be much broader because of this diversity of iron configrations with diffrent crossover pressures (Umemoto et al., 2008). Therefore, at lower-mantle conditions, bulk modulus, density, and bulk sound velocity should be in practice unaffected by the spin crossover. Nevertheless it could be worthwhile to investigate sound velocities in iron-bearing perovskite below room temperature, where the crossovers in ferrous and ferric iron should be sharper and possibly detectable. Their detection could give reference points around which the thermodynamics of this system could be modeled.

Table 1
Calculated parameters of the third-order Birch-Murnaghan equations of state. Note that these are static results and vibrational effects were not included in the calculation. Experimental values are for 15% iron concentration and taken from Lundin et al. (2008).

	V_0 (a.u.^{3}/(Mg, Fe)SiO_3)	K_0 (GPa)	K_0'
HS	271.93	262	3.9
IS	271.38	261	3.9
LS	270.89	259	4.0
MS at 300 K	271.55	273	3.6
MS at 2000 K	271.78	266	3.8
Exp.	275.50	257	4.0

Acknowledgments

Calculations were performed using the Quantum-ESPRESSO package (Giannozzi et al., 2009) at the Minnesota Supercomputing Institute and at the Indiana University's BigRed system. This research was primarily supported by EAR-0635990, EAR-0810272, ATM-0428774 (VLab), EAR-0757903. It was partially supported by the MRSEC Program of the National Science Foundation under award number DMR-0212302.

References

Badro, J., Rueff, J.P., Vankó, G., Monaco, G., Fiquet, G., Guyot, F., 2004. Electronic transitions in perovskite: possible nonconvecting layers in the lower mantle. Science 305, 383–386.
Bengtson, A., Persson, K., Morgan, D., 2008. *Ab initio* study of the composition dependence of the pressure-induced spin crossover in perovskite (Mg_{1-x},Fe_x)SiO_3. Earth Planet. Sci. Lett. 265, 535–545.
Bengtson, A., Li, J., Morgan, D., 2009. Mössbauer modeling to interpret the spin state of iron in (Mg, Fe)SiO_3 perovskite. Geophys. Res. Lett. 36, L15301.
Brown, J.M., Shankland, T.J., 1981. Thermodynamic parameters in the Earth as determined from seismic profiles. Geophys. J. R. Astron. Soc. 66, 579–596.
Burns, R.G., 1993. Mineralogical Applications of Crystal Field Theory. Cambridge University Press.
Caracas, R., Cohen, R.E., 2005. Effect of chemistry on the stability and elasticity of the perovskite and post-perovskite phases in the $MgSiO_3$–$FeSiO_3$–Al_2O_3 system and implications for the lowermost mantle. Geophys. Res. Lett. 32, L16310.
Cohen, R.E., Mazin, I.I., Isaak, D.G., 1997. Magnetic collapse in transition metal oxides at high pressure: implications for the earth. Science 275, 654–657.
Crowhurst, J.C., Brown, J.M., Goncharov, A.F., Jacobsen, S.D., 2008. Elasticity of (Mg, Fe)O through the spin transition of iron in the lower mantle. Science 319, 451–453.

Fei, Y., Zhang, L., Corgne, A., Watson, H., Ricolleau, A., Meng, Y., Prakapenka, V., 2007. Spin transition and equations of state of (Mg, Fe)O solid solutions. Geophys. Res. Lett. 34, L17307.

Giannozzi, P., et al., 2009. QUANTUM-ESPRESSO: a modular and open-source software project for quantum simulations of materials. J. Phys.: Condens. Matter 21, 395502, http://www.quantum-espresso.org.

Hsu, H., Umemoto, K., Blaha, P., Wentzcoitch, R., Spin states and hyperfine interactions of iron in (Mg, Fe)SiO_3 perovskite under pressure (submitted).

Hofmeister, A.M., 2006. Is low-spin Fe^{2+} present in Earth's mantle? Earth Planet. Sci. Lett. 243, 44–52.

Jackson, J.M., Sturhahn, W., Shen, G., Zhao, J., Hu, M.Y., Errandonea, D., Bass, J.D., Fei, Y., 2005. A synchrotron Mössbauer spectroscopy study of (Mg, Fe)SiO_3 perovskite up to 120 GPa. Am. Mineral. 90, 199–205.

Katsura, T., Sato, K., Ito, E., 1998. Electrical conductivity of silicate perovskite at lower-mantle conditions. Nature 395, 493–495.

Kiefer, B., Stixrude, L., Wentzcovitch, R.M., 2002. Elasticity of (Mg, Fe)SiO_3-perovskite at high pressures. Geophys. Res. Lett. 29, L14683.

Li, J., Struzhkin, V.V., -k Mao, H., Shu, J., Hemley, R.J., Fei, Y., Mysen, B., Dera, P., Prakapenka, V., Shen, G., 2004. Electronic spin state of iron in lower mantle perovskite. Proc. Natl. Acad. Sci. 101, 14027–14030.

Li, L., Brodholt, J.P., Stackhouse, S., Weidner, D.J., Alfredsson, M., Price, G.D., 2005. Electronic spin state of ferric iron in Al-bearing perovskite in the lower mantle. Geophys. Res. Lett. 32, L17307.

Lin, J.F., Struzhkin, V.V., Jacobsen, S.D., Hu, M.Y., Chow, P., Kung, J., Liu, H., Mao, H.K., Hemley, R.J., 2005. Spin transition of iron in magnesiowüstite in the Earth's lower mantle. Nature 436, 377.

Lin, J.F., Vankó, G., Jacobsen, S.D., Iota, V., Struzhkin, V.V., Prakapenka, V.B., Kuznetsov, A., Yoo, C.S., 2007. Spin transition zone in Earth's lower mantle. Science 317, 1740–1743.

Lin, J.F., Watson, H., Vankó, G., Alp, E.E., Prakapenka, V.B., Dera, P., Struzhkin, V.V., Kubo, A., Zhao, J., McCammon, C., Evans, W.J., 2008. Intermediate-spin ferrous iron in lowermost mantle post-perovskite and perovskite. Nat. Geosci. 1, 688–691.

Lundin, S., Catalli, K., Santillan, J., Shim, S.-H., Prakapenka, V.B., Kunz, M., Meng., Y., 2008. Effect of Fe on the equation of state of mantle silicate perovskite over 1 Mbar. Phys. Earth Planet. Int. 168, 97–102.

Mao, W.L., Meng, Y., Shen, G., Prakapenka, V.B., Campbell, A.J., Heinz, D.L., Shu, J., Caracas, R., Cohen, R.E., Fei, Y., Hemley, R.J., Mao, H.K., 2005. Iron-rich silicates in the Earth's D" layer. Proc. Natl. Acad. Sci. 102, 9751–9753.

McCammon, C., Kantor, I., Narygina, O., Rouquette, J., Ponkratz, U., Sergueev, I., Mezouar, M., Prakapenka, V., Dubrovinsky, L., 2008. Stable intermediate-spin ferrous iron in lower-mantle perovskite. Nat. Geosci. 1, 684–687.

Ono, S., Oganov, A.R., 2005. In situ observations of phase transition between perovskite and $CaIrO_3$-type phase in $MgSiO_3$ and pyrolitic mantle composition. Earth Planet. Sci. Lett. 236, 914–932.

Perdew, J.P., Zunder, A., 1981. Self-interaction correction to density-functional approximations for many-electron systems. Phys. Rev. B 23, 5048.

Stackhouse, S., Brodholt, J.P., Dobson, D.P., Price, G.D., 2006. Electronic spin transitions and the seismic properties of ferrous iron-bearing $MgSiO_3$ post-perovskite. Geophys. Res. Lett. 33, L12S03.

Stackhouse, S., Brodholt, J.P., Price, G.D., 2007. Electronic spin transitions in iron-bearing $MgSiO_3$ perovskite. Earth Planet. Sci. Lett. 253, 282–290.

Sturhahn, W., Jackson, J.M., Lin, J.F., 2005. The spin state of iron in minerals of Earth's lower mantle. Geophys. Res. Lett. 32, L12307.

Tateno, S., Hirose, K., Sata, N., Ohishi, Y., 2007. Solubility of FeO in (Mg, Fe)SiO_3 perovskite and the post-perovskite phase transition. Phys. Earth Planet. Int. 160, 319–325.

Tsuchiya, T., Wentzcovitch, R.M., da Silva, C.R.S., de Gironcoli, S., 2006. Spin transition in magnesiowüstite in Earth's lower mantle. Phys. Rev. Lett. 96, 198501.

Tsuchiya, T., Tsuchiya, J., 2006. Effect of impurity on the elasticity of perovskite and postperovskite: Velocity contrast across the postperovskite transition in (Mg,Fe,Al)(Si,Al)O_3. Geophys. Res. Lett. 33, L12S04.

Umemoto, K., Wentzcovitch, R.M., Yu, Y.G., Requist, R., 2008. Spin transition in (Mg, Fe)SiO_3 perovskite under pressure. Earth Planet. Sci. Lett. 276, 198–206.

Vanderbilt, D., 1990. Soft self-consistent pseudopotentials in a generalized eigenvalue formalism. Phys. Rev. B 41, R7892.

Wentzcovitch, R.M., 1991. Invariant molecular-dynamics approach to structural phase transitions. Phys. Rev. B 44, 2358.

Wentzcovitch, R.M., Martins, J.L., Price, G.D., 1993. Ab initio molecular dynamics with variable cell shape: application to $MgSiO_3$. Phys. Rev. Lett. 70, 3947.

Wentzcovitch, R.M., Justo, J.F., Wu, Z., da Silva, C.R.S., Yuen, D.A., Kohlstedt, D., 2009. Anomalous compressibility of ferropericlase throughout the iron spin crossover. Proc. Natl. Acad. Sci. 106, 8447–8452.

Wu, Z., Justo, J.F., da Silva, C.R.S., de Gironcoli, S., Wentzcovitch, R.M., 2009. Anomalous thermodynamics properties of ferropericlase throughout its spin crossover transition. Phys. Rev. B 80, 014409.

Xu, Y., McCammon, C., Poe, B.T., 1998. The effect of alumina on the electrical conductivity of silicate perovskite. Science 282, 922–924.

Zhang, F., Oganov, A.R., 2006. Valence state and spin transitions of iron in Earth's mantle silicates. Earth Planet. Sci. Lett. 249, 436–443.